International Journal for Housing Science and Its Applications
Publish August 10, 2025. Volume 46, Issue 4 Pages 3215-3230

https://doi.org/10.70517/ijhsa464266

Research on Intelligent Planning Algorithm of Electro-Hydrogen Coupling System for Complex Scenarios

Feng Zhao[1], Lingyue Kou[1], Jie Zhou[1,*], Chao Sun[1], Yiming Zhao[2] and Xiaoyu Wang[2]
[1] State Grid Jibei Electric Power Co. Ltd., Beijing, 100054, China
[2] State Grid Jibei Electric Power Research Institute, Beijing, 100054, China
Corresponding authors: (e-mail: jiezhou_buaa@163.com).

Abstract As a high-quality secondary energy carrier, hydrogen has application value in many aspects such as power generation, heat production, industry and transportation, especially in the field of difficult electrification and decarbonization, hydrogen becomes an inevitable choice of energy carrier in the future energy system and provides a good opportunity for the development of electric-hydrogen energy system. This paper explores the development of hydrogen energy and the demonstration application of electric-hydrogen coupling, and proposes three applicable scenarios for electric-hydrogen coupling application. Based on the concept of energy bus, the architecture of the coupling relationship between various devices in EH-IES is proposed and a mathematical model is established. The supply and demand balance of hydrogen load is realized by rationally arranging the output situation of each system, and then quantifying the characteristic indexes of grid operation, designing relevant objective functions and constraints, and solving the model using the improved scenario method. Analyzing the typical daily output of the system operation, the battery charging and the power input from the electrolyzer contribute 886.36kW and 1011.51kW respectively in the time period of 1:00-07:00.Comparing the operating costs of the three scenarios of the hydrogen refueling station, countryside, and industrial parks, in Scenario 2, the cost of the purchased power and the total revenue are 378,466 yuan respectively, 461654 yuan, the cost of purchased power increases dramatically, and the total benefit also decreases dramatically.

Index Terms Electric-hydrogen coupling, Energy bus, Load supply-demand balance, Objective function, Improved scenario approach

I. Introduction

The “dual-carbon target” has made it clear that new energy sources will play a major role in the future power system, and China's wind and photovoltaic power generation capacity will steadily increase in the future development process. A high proportion of new energy access has gradually become a basic feature of the new power system, but due to the shortcomings of new energy, such as volatility, randomness, intermittency, etc., it causes large-scale power abandonment problems [1]-[3]. Hydrogen energy has attracted much attention due to its unique inter-temporal flexibility, especially in the power and electricity imbalance problem caused by the increase in the installed share of new energy sources, hydrogen energy shows great potential [4]. Hydrogen energy system can convert excess renewable energy into “green hydrogen” and feed back to the grid through hydrogen fuel cell power generation, which not only helps to alleviate short-term power fluctuations and improve the stability of the grid, but also copes with the seasonal imbalance between supply and demand between sources and loads to ensure the reliability of energy supply [5]-[8]. In addition, hydrogen energy can be converted into multiple energy forms, which enhances the coupling relationship between integrated energy systems and promotes the efficient utilization and synergistic development of energy [9], [10].

With the large-scale access of electrolysis hydrogen system and the development and maturity of multiple hydrogen energy utilization technology, the impact of renewable hydrogen energy on the new energy-led power system generation, transmission, distribution, and use of each link will gradually appear [11], [12]. Hydrogen energy has a rich source, pollution-free, etc., its energy density, low carbon green, storage time and other aspects of the existence of advantages in the consumption of new energy, the economy of large-scale energy storage, storage and transportation mode of flexibility are better than other energy storage methods [13]-[16]. Reasonable planning and design of renewable hydrogen integrated energy system, to achieve synergistic optimization control and safe and economic operation, and at the same time accelerate the decarbonization process of industries with high carbon reduction difficulty, which is an important driving force for the scientific construction of a new type of power system and modern energy system [17]-[20].

Some scholars have analyzed the capacity optimization model of electric-hydrogen energy storage system by integrating the economic cost and new energy consumption capacity. Literature [21] constructed a coupled electric and thermal energy system with a hydrogen storage unit, gave full play to the advantages of hydrogen energy storage to realize the synergistic and efficient use of electric and thermal energy, and proposed the optimization strategy of the integrated energy system with hydrogen storage to further improve the energy efficiency level of the energy storage system. Literature [22] studied the P2HH model with start-stop characteristics and the seasonal hydrogen storage model, and used stochastic and robust optimization methods to plan the capacity allocation for the power load uncertainty problem. Literature [23] showed that electric hydrogen (PtH) generating units are characterized by flexible loads in the power system, and a mixed-integer linear programming model of the PtH unit considering the effect of temperature can help to measure the efficiency between power input and hydrogen production. Literature [24] proposes a shared hybrid electric-hydrogen energy storage system in the context of energy structure transformation and sharing economy development, using the microgrid two-layer optimal configuration method to solve the shared energy storage problem among multiple microgrids, which effectively promotes the efficient use of energy. Literature [25] examined the power system coordination and planning problem based on industrial hydrogen loads, effectively balancing the relationship between new energy consumption capacity and power system economic efficiency. The literature verified that the rational allocation of electric-hydrogen coupling system capacity through the establishment of relevant models can effectively improve the economy of the system and better realize the consumption of new energy.

The introduction of intelligent planning algorithms is the key to ensure the safe, economic and efficient operation of the electric-hydrogen integrated energy system. Literature [26] proposes a two-layer model for optimizing the capacity allocation and operation of electric-hydrogen coupled system, which takes the maximum economic efficiency as the typical scenario of capacity allocation, and realizes the maximum economic effect of the multi-energy coupled system under the solution of GUROBI and MOBWO-VIKOR methods by taking the operating characteristics analysis of the power system as the condition. Literature [27] constructed a framework of AC/DC electric-hydrogen coupled hybrid system for port areas, proposed an optimization model for equipment capacity allocation based on considering multiple types of hydrogen load plating, and solved it with GUROBI to achieve a low-cost and low-carbon emission energy management scheme. Literature [28] proposed a short time-scale energy management method based on physical model-assisted deep reinforcement learning for the problems of equipment nonlinear characteristics and stochastic generation of renewable energy sources that occur in industrial electric-hydrogen coupled systems, which demonstrated reliability in terms of improving the training efficiency, optimizing equipment scheduling as well as reducing the operating cost. Literature [29] emphasized that the hydro-hydrogen system is an ideal solution to promote the utilization of hydropower and the application of hydrogen energy, and established a two-layer planning model to maximize the system revenue, and solved the optimal capacity planning scheme for the hydro-hydrogen system by using the particle swarm optimization (PSO) algorithm and the Cplex as a means. Literature [30] designed a shared energy storage framework considering hydrogen trading, combining particle swarm optimization and mixed integer linear programming algorithms to solve the established hierarchical optimal scheduling model, which significantly improves the utilization of renewable energy resources while reduces the operating costs of each system. However, most of the above studies are typical or specific scenarios, and less consideration is given to the influence of the operating characteristics of hydrogen energy systems in complex scenarios on the planning results of electric-hydrogen coupled systems. Therefore, there is an urgent need to establish an intelligent planning algorithm for electric-hydrogen coupled system for complex scenarios, which can help to accurately portray the operating state of hydrogen energy system under complex scenarios, and then improve the effectiveness of the planning results of the electric-hydrogen coupled system, and promote the efficient utilization of the hydrogen energy system and the sustainable development of the system.

This paper proposes a new electric-hydrogen coupling system for the supply-demand balance and safe operation of new energy power generation systems, and clarifies the operation planning of electric-hydrogen coupling in three typical application scenarios, namely, hydrogen refueling stations, villages and industrial parks. The mathematical models of wind power, photovoltaic power generation, electrolysis, and hydrogen storage system in the system are constructed, and the objective function is designed, based on the formula of unit output, so as to calculate the characteristic indexes of grid operation, such as electricity and power generation cost. The constraints are used to optimize the solution process of the grid operation characteristic indexes. The linearization method is used to convert the constraints into a linear form, and the improved scenario method is introduced to reduce the computational difficulty of the long-term optimal operation problem to solve the model. And the operation of the system as well as the optimized dispatching results are analyzed through the arithmetic examples.

II. Electrohydrogen coupling system concept

II. A. Novel electrohydrogen coupling system

Aiming at the challenges brought by the high proportion of new energy generation to the system power balance and safe and stable operation, this paper proposes a new type of electric-hydrogen coupling system. Taking the high proportion of new energy consumption and high reliability operation of the power system as the goal, the new energy will be collected and connected to the DC transmission network which has no electrical connection with the AC power grid, and the mode of “off-grid transmission of green power at the sending end - off-grid hydrogen production at the receiving end - grid-connected hydrogen and gas power generation” will be adopted, so as to form an independent electric power system with the green hydrogen preparation as the core load and a regional fuel market using hydrogen as the medium, which will eliminate a large amount of new energy based on electricity-hydrogen-electricity conversion and bring about the challenges of power balance and safe and stable operation. Based on the electricity-hydrogen-electricity conversion, it decouples the large amount of new energy consumption and new “West-East Electricity Sending” demand from the sending/receiving end of the power system, gives full play to the functions of seasonal energy storage and power supply guarantee of hydrogen energy, and improves the level of security and stability of the electric power system and reduces the cost of the new energy system, guaranteeing a trillion dollars' worth of new energy system and ensuring that the new energy system can be used for a long time. It will meet the needs of large-scale new energy consumption, improve the security and stability of the power system, reduce the cost of the new energy system, and ensure the continued functioning of the trillion-dollar grid assets.

II. B. Analysis of typical application scenarios of electrohydrogen coupling

Combining a series of supportive policies for the development of hydrogen energy and the current status of electric-hydrogen coupling demonstration applications, this paper summarizes three typical application scenarios of electric-hydrogen coupling in hydrogen refueling stations, villages, and industrial parks [31].

II. B. 1) Integrated hydrogen production and refueling stations

Integrated hydrogen production and refueling refers to the construction method of hydrogen production and refueling in which hydrogen production equipment is set up in the hydrogen refueling station, and after the hydrogen is prepared and purified by the purification system, the hydrogen is passed into the compressor and stored for refueling to the refueling vehicle.

II. B. 2) Water-photovoltaic-electricity-hydrogen-biomass integrated utilization rural scenarios

Water-Photovoltaic-Electricity-Hydrogen-Biomass is to comprehensively utilize the abundant hydropower, photovoltaic and biomass resources in the countryside, build a multi-energy conversion system with electricity as the core, realize hydrogen production from hydropower and gas production from biomass, satisfy the demand for diversified energy use in buildings, transportation and industry, and in-depth decarbonization, and promote local consumption of surplus hydropower and the recycling of rural wastes.

II. B. 3) Electricity-Hydrogen-Heat-Vehicle Coupled Hydrogen Energy Industrial Parks

Typical application of electricity-hydrogen-heat-vehicle coupling hydrogen energy industrial park refers to the hydrogen energy industrial park, giving full play to the advantages of the industry, utilizing renewable energy to generate electricity, electrolysis of water to produce hydrogen, hydrogen storage, hydrogen fuel cell vehicle hydrogen refueling, hydrogen fuel cell combined heat and power supply and other links, to meet the user's multiple energy needs for electricity, hydrogen and heat.

III. Modeling of electrohydrogen coupled systems and equipment

III. A. Electric-Hydrogen Coupling System Architecture

In this paper, the coupling relationship between various types of equipment in the EH-IES is described in detail based on the concept of energy bus [32]. The system not only includes traditional power system equipment such as power grids and new energy generation facilities, but also covers hydrogen energy system equipment such as electrolyzers, hydrogen fuel cells, hydrogen storage tanks, and pressure conversion devices. This comprehensive layout effectively integrates the hydrogen production, storage, and utilization segments, forming a fully functional regional-level electric-hydrogen integrated energy system, as shown in Fig. 1.

(1) Direct supply: Hydrogen is pressurized by a compressor and injected into a high-pressure storage tank and subsequently supplied to a hydrogen refueling station.

(2) Long-term storage: Hydrogen is pressurized by compressors and injected into low-pressure hydrogen storage tanks for long-term and large-scale storage.

(3) Hydrogen to electricity: Hydrogen is used to generate electricity through hydrogen fuel cells.

(4) Hydrogen to gas: Hydrogen reacts with carbon dioxide in the methanization equipment under the action of a catalyst to produce methane and inject it into the gas grid. The electrical load of the system is supplied by the combination of photovoltaic, wind power, hydrogen fuel cells and the upper grid, the hydrogen load is supplied by the hydrogen produced in the electrolyzer and the hydrogen stored in the storage tanks, and the gas load is supplied by the methanization equipment and the gas grid. The hydrogen energy system is tightly coupled with multiple energy systems in the region through electrolyzers, hydrogen fuel cells, methanization equipment and hydrogen storage tanks.

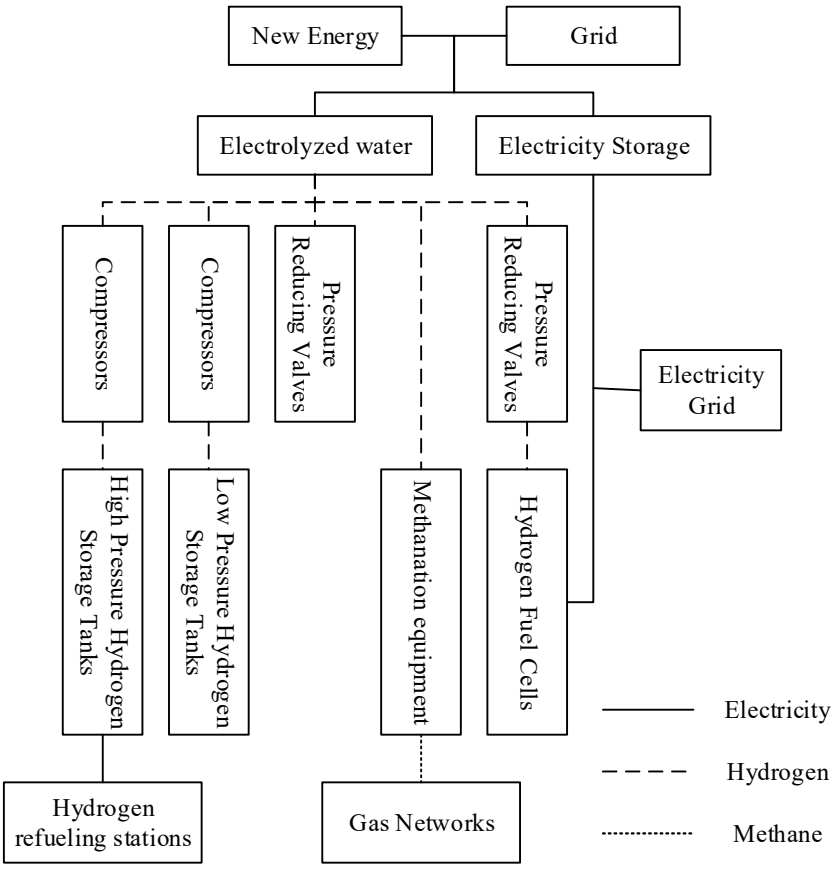

Figure 1: The regional level of the hydrogen integrated energy system

III. B. Modeling of system equipment

III. B. 1) Wind power modeling

The wind turbine output power is related to the real-time wind speed, and when the time lag effect and wake effect of the wind farm are not taken into account, the main relationship between the wind turbine output power and the wind speed can be expressed by a segmented function, which is mathematically modeled as follows [33]:

$$P_{wird}=\begin{cases}0 & v_t<v_{in}\cup v_{out}<v_t\\ P_{wN}\dfrac{v_t^3-v_{in}^3}{v_r^3-v_{in}^3} & v_{in}\le v_t<v_r\\ P_{wN} & v_r\le v_t\le v_{out}\end{cases} \tag{1}$$

where P_{wird} is the actual power output of the fan, P_{wN} is the rated power output of the fan, v_t is the actual wind speed, v_r is the rated wind speed, v_{in} and v_{out} are the cut-in and cut-out wind speeds, respectively.

III. B. 2) Modeling of photovoltaic power generation

The theoretical output power of photovoltaic panels is related to the intensity of solar radiation, ambient temperature and other factors, and its mathematical model is:

$$P_{PV}=\begin{cases}P_{pN}D_t^2/D_{STC}/R_c\left[1+k_t\left(T_t-T_{ref}\right)\right] & D_i<R_c\\ P_{pN}D_t/D_{STC}\left[1+k_t\left(T_t-T_{ref}\right)\right] & D_i\geq R_c\end{cases} \tag{2}$$

where P_{PN} is the rated output power of the PV panel, D_1 is the actual radiation intensity, D_{STC} is the rated radiation intensity of the PV module test (generally $1\mathrm{kW/m^2}$), R_c is the radiation intensity at a fixed location, k_t is the temperature coefficient, T_t is the actual temperature, and T_{ref} is the test temperature.

III. B. 3) Electrolytic system model

The system power of the electrolysis system is a linear function of the electrolysis power, where the coefficients are related to the system size and configuration, while the hydrogen production rate is determined by the electrolysis power, and the mathematical model for both is:

$$\begin{aligned}p_{x,i}^H&=p_{aux,t}^H+\left(1+\alpha_{aux}^H\right)p_{m,t}^H\\ q_{m,t}^H&=\eta_{m,s}^H p_{m,t}^H/Q_{HHV}\end{aligned} \tag{3}$$

where $p_{s,t}^H$ is the power of the hydrogen production system, $p_{m,t}^H$ is the electrolysis power, $p_{a\times a}^H$ is the fixed power of the auxiliary engine, α_{aux}^H is the dynamic power coefficient of the auxiliary engine, $q_{m,t}^H$ is the hydrogen production rate, Q_{HRV} is the calorific value of hydrogen, and $\eta_{m,t}^H$ is the efficiency of hydrogen production by electrolysis.

III. B. 4) Modeling of hydrogen storage equipment

Hydrogen is generally stored using high-pressure tanks, and the amount of hydrogen stored at moment t depends on the amount of hydrogen stored at the previous moment and the amount of hydrogen fed and used at that moment, as modeled below:

$$\begin{aligned}m_{shot,t}^H&=m_{shot,t-1}^H+q_{mi,t}^H\Delta t-q_{ci,t}^H\Delta t\\ SOC_{sigi,t}^H&=m_{sigi,t}^H/M_{sigi}^H\end{aligned} \tag{4}$$

where $m_{sigi,t}^H$ is the hydrogen storage capacity of the tank at time t, $q_{ct,t}^H$ is the rate of hydrogen use, M_{sigi}^H is the rated storage capacity of the tank, and $SOC_{sigi,t}^H$ is the percentage of tank capacity.

III. C. Operational Optimization Model

III. C. 1) Objective function

The production simulation object is the operation characteristics of the power grid containing a high proportion of VRE power. By rationalizing generator output, wind power output, energy storage charging and discharging, and hydrogen production power, the total electric load and total power generation balance, hydrogen load supply and demand balance are realized, and the network transmission capacity constraints, as well as the standby constraints, ramp-up constraints, energy storage constraints, and hydrogen production and storage constraints are accounted for in the form of DC tidal current. Then, the network tidal current is calculated based on the unit output, which in turn calculates the power, VRE power, carbon emission, generation cost, and other grid operation characteristic indicators. Fuel, standby and start/stop costs of thermal units, carbon emission costs, penalty costs for load shedding and wind and solar abandonment, power purchase costs, and operating costs of the electrolysis system are considered [34]:

$$\begin{aligned}&\min_x f(x)\\ &where, f(x)=\sum_{t=1}^{t}C_{g,t}^G+C_t^{Fine}+C_t^{Ele}+C_t^{Ct}+C_{m,t}^H\end{aligned} \tag{5}$$

where, $C_{g,t}^G$ is the thermal power unit operation cost, C_t^{Fine} is the system operation penalty cost, C_t^{Ek} is the purchased power cost, and $C_{m,t}^H$ is the hydrogen production equipment operation and maintenance cost.

(1) Thermal power operation cost

Thermal power operation cost consists of coal consumption cost, rotating standby cost and start-stop cost, and its expression is as follows:

$$\begin{cases} C_{g,t}^{G} = \sum \left(C_{i,t}^{Ge} + C_{i,t}^{Gr} + C_{i,t}^{Gud} \right) \\ C_{i,t}^{Ge} = \left(c_{cool} + c_{Co2} F_{coal} \right) M_{i,t}^{C} \\ M_{i,t}^{C} = a_i^{G} \left(p_{i,t}^{G} \right)^2 + b_i^{G} p_{i,t}^{G} + c \\ C_{i,t}^{Gr} = c_i^{G+} r_{i,t}^{G+} + c_i^{G-} r_{i,t}^{G-} \\ C_{i,t}^{Gud} = c_i^{Gup} v_{i,t}^{G} + c_i^{Gitn} \omega_{i,t}^{G} \end{cases} \tag{6}$$

In the formula, $C_{i,t}^{GE}$, $C_{i,t}^{Gr}$ and $C_{i,t}^{Gd}$ are the coal consumption cost, rotating standby cost and start/stop cost of each thermal power unit, g is the number of thermal power units, $M_{i,l}^{C}$ is the coal consumption of thermal power units, and $p_{i,}^{G}$ is the power of the units. a_i^{G}, b_i^{G}, c_i^{G} are the coal cost coefficients of each thermal power unit, $r_{i,t}^{G+}$, $r_{i,t}^{G-}$ are the upper and lower standby capacities, $v_{i,t}^{G}$, $\omega_{i,t}^{G}$ are the startup and shutdown events, c_{cod} is the coal price, c_{CO2} is the carbon dioxide price, F_{coa} is the carbon emission factor of standard coal, c_i^{G+}, c_i^{G-} are the costs of upper and lower standby unit capacities, and c_T^{Gup}, c_l^{Gin} are the startup and shutdown costs.

(2) Penalty cost

In order to prevent load cutting and wind and light abandonment, the system operation penalty cost is set for load cutting, wind and light abandonment respectively, and its expression is as follows:

$$C_t^{Fine} = \sum_{i \in \Omega_j} c_i^{LD} p_{i,t}^{LD} + \sum_{i \in \Omega_s} c_i^{Wdr} p_{i,t}^{Wdr} + \sum_{i \in \Omega_v} c_i^{Vdr} p_{i,t}^{Vdr} \tag{7}$$

In the formula, p^{LD}, $p_{i,t}^{Wdr}$, $p_{i,t}^{Vdr}$ are the cut load power, abandoned wind power and abandoned light power, l, w, v are the cut load, the number of wind power and photovoltaic, c_t^{LD}, c_t^{Wdrop}, c_t^{Vdrop} are the unit cut load, abandoned wind and abandoned light cost.

(3) Power purchase cost

The power purchase cost of long-distance transmission is expressed as follows:

$$C_t^{Ek} = c_t^{cle} p_1^{E} \tag{8}$$

where p_t^{E} is the purchased power at the moment of t, and c_t^{cle} is the time-shared power purchase price.

(4) Operation and maintenance cost of hydrogen production

The operation cost of the hydrogen production system is mainly the operation and maintenance cost, which is expressed as follows:

$$C_{m,t}^{H} = \sum_{i \in \Omega_s} c^{Hop} p_{si,t}^{H} \tag{9}$$

where c^{Hap} is the O&M cost per unit of hydrogen production power.

III. C. 2) Constraints

(1) Power balance constraints

$$\sum_{i \in \Omega_t} p_{i,t}^{G} + \sum_{i \in a_{i,t}} p_{i,t}^{VRE} + p_t^{E} = \sum_{i \in \Omega_t} \left(p_{i,t}^{L} - p_{i,t}^{LD} \right) + \sum_{i \in \Omega_t} \left(p_{s,t}^{H} \right) \tag{10}$$

In the formula, $p_{i,t}^{G}$, $p_{i,t}^{VRE}$, p_t^{E} are the thermal power units, VRE units and remote power supply output in each time period, $p_{i,t}^{L}$, $p_{i,t}^{LD}$, $p_{ri,t}^{H}$ are the loads, cut loads, and power of the electric hydrogen production system, respectively.

(2) Line current constraint (DC current)

$$P_{i\min}^{line} \le P_{i,t}^{line} \le P_{i\max}^{line} \tag{11}$$

where, $P_{i,t}^{line}$, $P_{i\ \min}^{line}$ and $P_{i\max}^{line}$ are the real time line currents, line minimum and maximum currents.

(3) Rotating standby demand constraint

$$\begin{cases} \sum_{i\in\Omega_s} r_{j,}^{G+} \geq \sum_{k\in\Omega_s} p_{k,t}^{L} \times L^{+}\% + \sum_{j\in\Omega_{VRE}} p_{j,t}^{VRE} \times W^{+}\% \\ \sum_{i\in\Omega_s} r_{i,l}^{G-} \geq \sum_{k\in\Omega_s} p_{k,t}^{L} \times L^{-}\% + \sum_{j\in\Omega_{VRE}} p_{j,t}^{VRE} \times W^{-}\% \end{cases} \tag{12}$$

where, L^{+}, L^{-}, W^{+}, W^{-} are the standby requirement coefficients for load and VRE unit output margin respectively.

(4) Thermal power unit constraints

Output constraint:

$$u_{i,t}^{G} P_{i\min}^{G} \leq p_{i,t}^{G} \leq u_{i,t}^{G} P_{i\max}^{T} \tag{13}$$

where $P_{\min}^{G}$ and $P_{\max}^{G}$ are the minimum and maximum output of the conventional unit: $u_{i,t}^{G}$ is the unit state (1 for operation and 0 for shutdown).

Standby constraints:

$$\begin{cases} p_{i,t}^{G} + r_{i,t}^{G+} \leq u_{i,t}^{G} P_{t\max}^{G} \\ p_{i,t}^{G} - r_{i,t}^{G-} \geq u_{i,t}^{G} P_{t\min}^{G} \end{cases} \tag{14}$$

Climbing constraints:

$$\begin{cases} p_{i,t}^{G} - p_{i,t-1}^{G} \leq D_{i}^{G+} \\ p_{i,t-1}^{G} - p_{i,t}^{G} \geq D_{i}^{G-} \end{cases} \tag{15}$$

where D_{i}^{G+} and D_{i}^{G-} are the upward and downward power variations of the conventional unit at operating hours.

(5) VRE unit output and purchased power constraints

$$\begin{cases} 0 \leq p_{i,t}^{VRE} \leq P_{i\max}^{PRE} \\ 0 \leq p_{t}^{E} \leq P_{\max}^{E} \end{cases} \tag{16}$$

where $P_{\max}^{VRE}$ is the maximum output of the VRE unit and $P_{\max}^{E}$ is the maximum purchased power.

(6) Electrolysis system constraints

Output power constraint:

$$\begin{cases} p_{si,t}^{H} = u_{i,t}^{H} p_{auxi,t}^{H} + \left(1+\alpha_{aux,i}^{H}\right) p_{mi,t}^{H} \\ u_{i,1}^{H} P_{mi\min}^{H} \leq p_{mi,t}^{H} \leq u_{i,t}^{H} P_{mi\max}^{H} \end{cases} \tag{17}$$

where $P_{mi\min}^{H}$, $P_{mi\max}^{H}$ are the minimum and maximum operating power of the electrolyzer, and $u_{i,t}^{H}$ is the unit state (1 for operation and 0 for shutdown).

Climbing constraints:

$$\begin{cases} p_{mi,t}^{H} - p_{mi,t-1}^{H} \leq u_{i,t-1}^{H} P_{i\max}^{H+} \\ p_{mi,t-1}^{H} - p_{mi,t}^{H} \geq u_{i,j}^{H} P_{i\max}^{H-} \end{cases} \tag{18}$$

where $P_{mi\max}^{H}$, $P_{mi\max}^{H}$ are the maximum limits of upward and downward climb of the electrolyzer, respectively.

(7) Hydrogen storage capacity constraint

$$\begin{cases} SOC_{sigi\min}^{H} \leq SOC_{stgi,t}^{H} \leq SOC_{sigi\max}^{H} \\ SOC_{sigi,i0}^{H} = SOC_{stgi,read}^{H} \end{cases} \tag{19}$$

where $SOC_{sigi\min}^{H}$ and $SOC_{sigi\max}^{H}$ are the minimum and maximum storage capacity percentages of the hydrogen storage tanks, respectively. To ensure that the hydrogen storage system meets the operating conditions of each

cycle, the initial state of the hydrogen storage SOC in the operating cycle is constrained to be equal to the termination state in the optimization.

In the optimization solution process, only consider the above constraints can not complete the solution calculation, need to consider the network interconnection and the dynamic conditions of the equipment operation constraints, for this reason, will be the DC current, thermal power unit start-stop and electrolysis system start-stop constraints of the further processing of the elaboration is as follows.

III. D. Model solving method based on improved scenario approach

The planning problem is a large-scale nonlinear optimization problem involving a large number of decision variables, so it is very difficult to solve the planning model of the electric-hydrogen coupled system considering the characteristics of multiple operating conditions. In order to reduce the computational difficulty of the planning problem, this section first adopts the introduction of auxiliary variables and linearizes the nonlinear terms in the model by the large M method, and then simplifies the above model by the improved scenario method.

III. D. 1) Modeled linearization methods

Due to the existence of nonlinear term forms in the above model, it is more difficult to solve it directly. In order to reduce the difficulty of solving, this paper adopts the linearization method to linearize it. For different nonlinear terms in the model, the following method is used to linearize the model.

Introduce auxiliary variable $P_{s,t}^{ED,aux}$ and make it satisfy the following constraints:

$$\begin{cases} P^{ED,rated} - \left(1-u_{s,t}^{ED}\right) P_{\max}^{ED,rated} \le P_{s,t}^{ED,aux} \\ \le P^{ED,rated} - \left(1-u_{s,t}^{ED}\right) P_{\min}^{ED,ruted} \\ u_{s,t}^{ED} P_{\min}^{ED,rated} \le P_{s,t}^{ED,aux} \le u_{s,t}^{ED} P_{\max}^{ED,rated} \end{cases} \tag{20}$$

Then the constraint can be rewritten in the following linear form:

$$w_{s,\min}^{ED} P_{s,t}^{ED,aux} \le P_{s,1}^{ED} \le w_{s,\max}^{ED} P_{s,t}^{ED,aux} \tag{21}$$

Similarly, the same linearization method can be used, rewritten in the following linear form:

$$w_{s,\min}^{FC} P_{x,t}^{FC,aux} \le P_{x,t}^{FC} \le w_{x,\max}^{FC} P_{s,i}^{FC,aux} \tag{22}$$

$$w_{x,\min}^{MR} P_{s,1}^{MR,aux} \le P_{x,1}^{MR} \le w_{s,\max}^{MR} P_{s,c}^{MR,\max} \tag{23}$$

$$\begin{aligned} 0 \le P_{k,t}^{/dil} \le w^{j} P_{k,t}^{j,dis,aux} \\ 0 \le P_{k,l}^{j,ch} \le w^{j} P_{k,l}^{j,ch,anx} \end{aligned} \tag{24}$$

First introduce auxiliary variable $C^{ED,inv,aux}$ and add constraints:

$$\begin{cases} -Mu_{x,l}^{ED} \le C^{ED,inv,aux} \le Mu_{s,t}^{ED} \\ C^{ED,inv} - M\left(1-u_{x,t}^{ED}\right) \le C^{ED,inv,aux} \\ \le C^{ED,inv} + M\left(1-u_{s,t}^{ED}\right) \end{cases} \tag{25}$$

where M is a large enough constant to be rewritten in the following linear form:

$$C_{t}^{ED,de} = \frac{C^{ED,inv,aux}}{T_{ED,ot}} \tag{26}$$

III. D. 2) Improvement of the scenario method

The long-term optimal running problem is a large-scale mixed-integer optimization problem involving a large number of decision variables, which makes the above model very difficult to solve. In order to reduce the computational difficulty of the long-run optimization problem, this section adopts the improved scenario method to simplify the above model [35].

(1) Concept of improved scenario method

Improved Scenario Approach is based on the traditional scenario analysis method, by modeling and characterizing the states “within a single typical scenario” and “multiple typical scenarios coupled”, thus overcoming

the shortcomings of the traditional scenario analysis method, which is only applicable to the operation and planning analysis “within a single typical scenario”, and greatly reducing the computational complexity. The traditional scenario analysis method only applies to the operation and planning analysis of “a single typical scenario”, and significantly reduces the computational complexity. In this paper, the typical scene time scale is taken as 24h a day, i.e. typical day.

(2) Low-pressure hydrogen storage tank operation model based on scenario coupling

Since low-pressure hydrogen storage tanks can operate in a long time scale, it is necessary to consider not only the temporal coupling characteristics of low-pressure hydrogen storage tanks within the day, but also the correlation between low-pressure hydrogen storage tanks between the days.

The intra-day hydrogen storage capacity of the low-pressure hydrogen storage tank is:

$$\begin{aligned} m_{k,t+1}^{LHS,\text{int}ra} &= \left(1-\eta^{LHS,loss}\Delta t\right) m_{k,t}^{LHS,\text{int}ra} \\ &+\left(\eta^{LHS,in} m_{k,t}^{LHS,\text{int}ra,in} - \frac{m_{k,t}^{LHS,\text{int}ra,out}}{\eta^{LHS,out}}\right)\Delta t \end{aligned} \tag{27}$$

$$m_{k,t,,\text{int}ra}^{LH} = 0 \tag{28}$$

$$0 \le m_{k,t}^{LH\,\text{Sin}tra,in} \le B_{k,t}^{LHS,in} S^{LHS,rated} \tag{29}$$

$$0 \le m_{k,t}^{LH\,\text{Sin}tra,out} \le B_{k,t}^{LHS,out} S^{LHS,rated} \tag{30}$$

$$B_{k,t}^{LHS,in} + B_{k,t}^{LHS,out} \le 1 \tag{31}$$

where, $m_{k,t}^{LHS,\text{int}ra}$ for a typical day k moments t of the intraday hydrogen storage, $\eta^{LHS,loss}$, $\eta^{LHS,in}$, $\eta^{LHS,out}$, respectively, for low-pressure hydrogen storage tank hydrogen storage self-loss rate, hydrogen charging loss and release loss, $m_{k,t}^{LHS,\text{int}ra,in}$, $m_{k,t}^{LHS,\text{int}ra,out}$, respectively, for low-pressure hydrogen storage tank intraday hydrogen storage, hydrogen release, $B_{k,t}^{LHS,in}$, $B_{k,t}^{LHS,out}$, respectively, for a typical day k moments t of the low-pressure hydrogen storage tank hydrogen storage, release of the state of the variable, $S^{LHS,rated}$ for the planning of low-pressure hydrogen storage tank capacity.

Low-pressure hydrogen storage tanks in the initial moment of the day the mass of stored hydrogen to meet the following constraints:

$$m_{r+1}^{LHS,\text{int}ra} = \left(1-\eta^{LHS,loss}\Delta t\right)^{N_t} m_r^{LHS,\text{int}ra} + m_{k=h(r),N_t+1}^{LHS,\text{int}ra} \tag{32}$$

$$m_{N_t+1}^{LHS,\text{int}ra} = m_1^{LHS,\text{int}ra} \tag{33}$$

where $m_{r+1}^{LHS,\text{int}ra}$ is the initial moment of hydrogen storage on operating day $r+1$, N_t is the total moments of an operating day, and $k=h(r)$ is the mapping factor between typical and operating days. Eq. (33) ensures that the capacity of the low-pressure hydrogen storage tank remains the same at the beginning and the end of the operating cycle.

Therefore, the mass of hydrogen stored in the low-pressure hydrogen storage tank can be expressed as:

$$m_{r,t}^{LHS} = m_r^{LHS,\text{int}ra} + m_{k=h(r),t}^{LHS,\text{int}ra} \tag{34}$$

where $m_{r,t}^{LHS}$ is the true mass of hydrogen stored in the low-pressure hydrogen storage tank for each operating day r moment t.

In order to guarantee the safe operation of hydrogen storage, the low-pressure hydrogen storage tank needs to satisfy the following constraints:

$$\begin{cases} m_k^{LHS,\text{int}ra,\max} \ge m_{k,t}^{LHS,\text{int}ra} \\ m_k^{LHS,\text{int}ra,\min} \le m_{k,t}^{LHS,\text{int}ra} \end{cases} \tag{35}$$

$$\begin{cases} m_r^{LHS,\text{int}ra} + m_{k=h(r)}^{LHS,\text{int}rax\max} \le \sigma_{\max}^{LHS} S^{LHS} \\ m_r^{LHS,\text{int}ra} + m_{k=h(r)}^{LHS,\text{int}a,\min} \ge \sigma_{\min}^{LHS} S^{LHS} \end{cases} \tag{36}$$

where $m_k^{LHS,\text{int}ra,\max}$ and $m_k^{LHS,\text{int}ra,\min}$ are the maximum and minimum intraday hydrogen storage mass of the LVH storage tank, $\sigma_{\min}^{LHS}$ and $\sigma_{\max}^{LHS}$ are the minimum and maximum hydrogen storage mass ratios of the LVH storage tank, and S^{LHS} is the planned capacity of the LVH storage tank.

IV. Analysis of examples

IV. A. Analysis of system operation

Figure 2 shows the output and load curves of each device in a typical day. In the 1:00-07:00 time period, the system load is low, and the system converts the excess power into hydrogen for storage through the alkaline electrolyzer in addition to energy storage through the battery, which greatly reduces the amount of wind and photovoltaic power discarded by the system. In this time period, the battery charging and the power input from the electrolyzer contribute 886.36kW and 1011.51kW respectively. 08:00-09:00 time period, as the new energy generation cannot meet the system load, the system load shortfall is made up by the battery discharging, and the average value of the discharged power is 1499.1kW. 12:00 -17:00 time period, the PV power generation is sufficient, there is a surplus capacity is stored by the hybrid energy storage system, but due to the limited capacity of the energy storage system, all accompanied by a small portion of the abandoned wind and photovoltaic power, the total energy of the abandoned wind and power is 2,462.4kW. 18:00-23:00 time period, the PV output is 0, and the system load is met partially by the storage battery and hydrogen fuel cells to meet part of the system load.

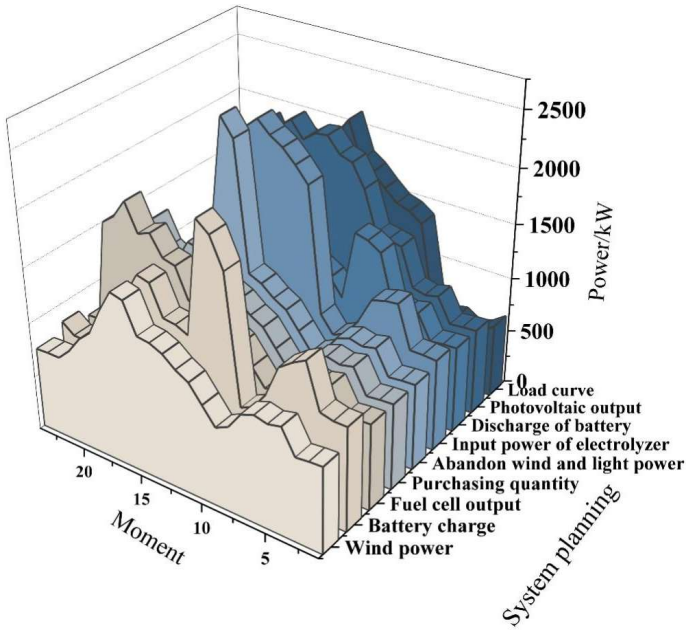

Figure 2: Typical daily output and load curves of each device

IV. A. 1) Typical scenarios of wind power outputs

Figure 3 shows the wind and solar power output in typical scenarios, with hydrogen refueling station in Figure (a), countryside in Figure (b), and industrial park in Figure (c). The three scenarios utilize different power generation situations. The hydrogen refueling station (Scenario 1) uses an adjustable operating power for both the electrolyzer and the hydrogen-to-ammonia production, i.e., the electrolyzer follows the new energy output, while considering the demand-side response of the hydrogen-to-ammonia production. Rural (Scenario 2): the electrolyzer cannot follow the new energy output, i.e., the electrolyzer is in constant power operation, and the hydrogen-to-ammonia operation power is adjustable. Industrial Park (Scenario 3): the demand-side response of hydrogen to ammonia is not considered, i.e., the hydrogen to ammonia is in constant power operation, and the electrolyzer operates with adjustable power. Simulation analysis is performed with EH-IES.

The peaks of new energy output in Fig. (a) are located in the morning at 07:00-09:00 hrs and in the afternoon at 15:00-17:00 hrs, and the peaks of power generation are 169.82 MW and 79.62 MW, respectively.During these hours, the supply of hydrogen refueling stations is greater than the demand, and sending a large amount of surplus power to the grid will bring a huge penalty cost. Therefore, in Scenario 1, the surplus power is converted into hydrogen through the electrolyzer to realize the consumption of new energy, especially at 09:00 when the total output of new

energy is the largest, and the hydrogen production of the electrolyzer reaches the maximum value (75.95MW), and at the same time the hydrogen ammonia production is running at the maximum power, so as to consume as much as possible the wind power and the photovoltaic. At 14:00 and 19:00, the new energy generation in the hydrogen refueling station is difficult to meet the load demand. Considering the high power purchase price at this time, purchasing power from the external grid will bring huge power purchase cost, which is not conducive to the maximization of the revenue of the hydrogen refueling station, therefore, the hydrogen refueling station uses hydrogen-fueled generators to generate power to satisfy the load demand at these two times. At the same time, in order to alleviate the pressure on the electric and hydrogen loads at these times, the hydrogen ammonia production is also operated at minimum power, thus significantly reducing the purchased power cost of the hydrogen refueling station.

In Scenario 2, the electrolyzer is in constant power operation. Most of the time, it generates electricity through hydrogen fuel, and the peak power is 100.44 WM and 100.84 WM at 14:00 and 18:00, respectively. When the new energy output is the largest, the power of the electrolyzer is too low to consume the excess new energy power, and when the load is the largest in the countryside, the electrolyzer can't reduce its own power, which increases the burden of the countryside's power purchasing instead. Under this operation mode, the power transactions between the countryside and the outside world are more frequent and the amount of traded power increases significantly, which is not conducive to the overall development of the countryside.

In Scenario 3, hydrogen-to-ammonia is in constant power operation, which does not provide adjustable and flexible type of resources for the park. For example, at 03:00-04:00, 11:00-15:00, and 18:00-22:00, when the renewable power output is in the trough, the output power is 30.64 WM, 33.09 WM, and 33.9 WM, respectively.Appropriately decreasing the production power of the hydrogen ammonia production can reduce the total load of the park and lower the cost of purchased power. At the peak of renewable power output at 09:00 (178.01WM), appropriately increasing the production capacity of hydrogen to ammonia is conducive to promoting the consumption of new energy and minimizing the abandonment of wind and light.

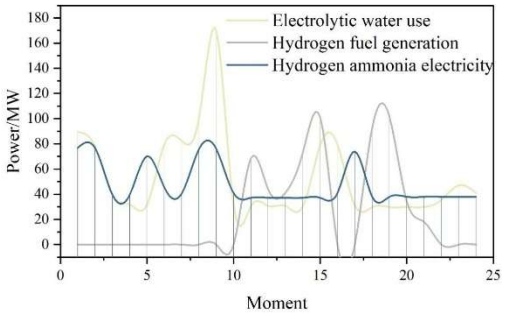

(a)Hydrogen refueling station

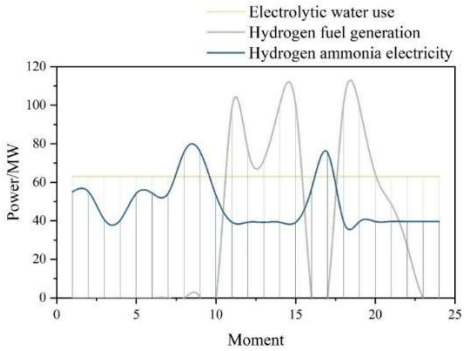

(b)The country

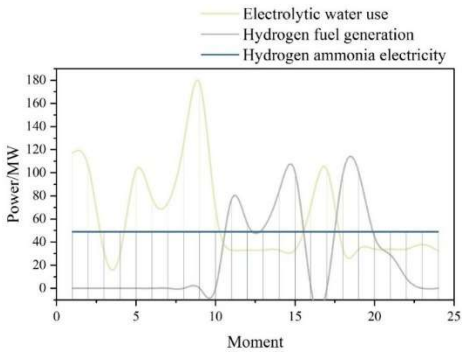

(c)The industrial park

Figure 3: Scenery output in typical scenes

IV. A. 2) Load curves

Latin hypercubic sampling is used to generate 1,000 scenarios of wind-scenic output for 168h at weekly time scales, and three groups of typical scenarios of wind-scenic output are obtained by scenario reduction with 168h loads, as shown in Fig. 4. The wind-scenic processing load has a cyclic pattern, with 24h as a cycle, and the peak occurs at the 13th hour of each cycle, which is 958.82kW.

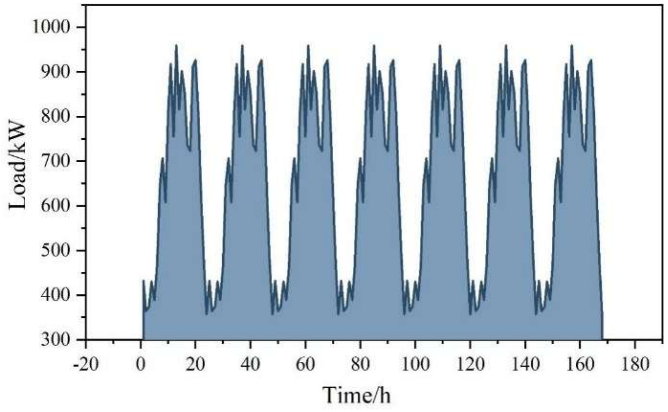

Figure 4: Load curve

IV. B. Analysis of two-phase multi-timescale optimization scheduling results

IV. B. 1) Optimization results in different scenarios

Figure 5 shows the charging and discharging of the battery for 168 h under three scenarios, with the positive value indicating the battery discharging state and the negative value indicating the charging state. Figure 6 shows the power purchase and sale of the system from the external grid under the three scenarios, the positive value indicates that the system purchases power from the external grid, and the negative value indicates that the system sells power to the external grid. Comparing the battery charging and discharging situation and the interaction between the system and the external grid in the three scenarios, the system in Scenario 1 completely relies on its own power storage device with the wind power to supply the load demand, and adjusts the power purchase and sale price according to the relationship between supply and demand and real-time purchase and sale of electricity and the interaction with the external grid, and most of the time, sells the power to the external grid, with the highest power sale of 950 kW. Scenario 2 joins the hydrogen storage in a short time scale, and the electricity and hydrogen can be adjusted appropriately through electric-hydrogen conversion. Scheduling strategy, the degree of dependence on the external grid is relatively reduced.

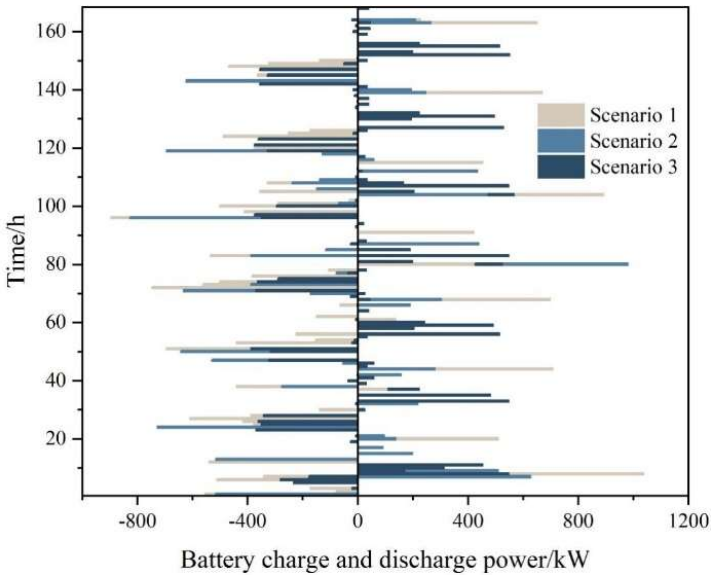

Figure 5: The charge of the battery 168 h under the scene

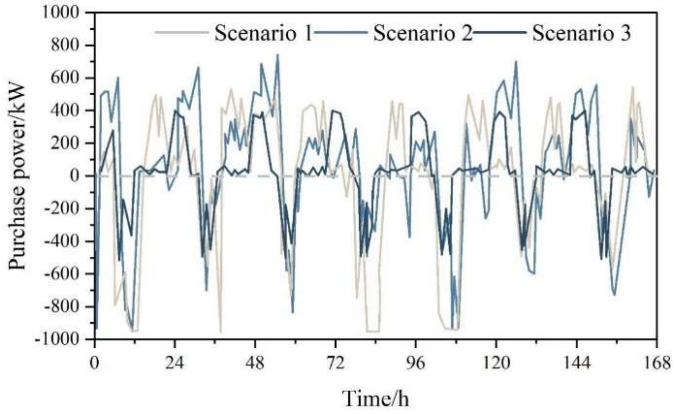

Figure 6: 3 scenarios of the system is sold from foreign electricity

IV. B. 2) Comparison of optimization economics in different scenarios

Figure 7 shows the comparison of the operating costs of the three scenarios. In Scenario 2, the frequent power trading leads to a significant increase in the power purchase cost of the countryside and a significant decrease in the total revenue, with the power purchase cost and total revenue being 378,466 yuan and 461,654 yuan, respectively. The comparison between Scenario 3 and Scenario 1 shows that when considering the demand-side response of hydrogen to ammonia production, the ammonia production revenue is basically unchanged, and at the same time, due to the inclusion of adjustable flexibility resources, it can make the power purchase cost and the cost of wind and light abandonment penalties decrease further, which in turn improves the total revenue of the park by about 21.49%.

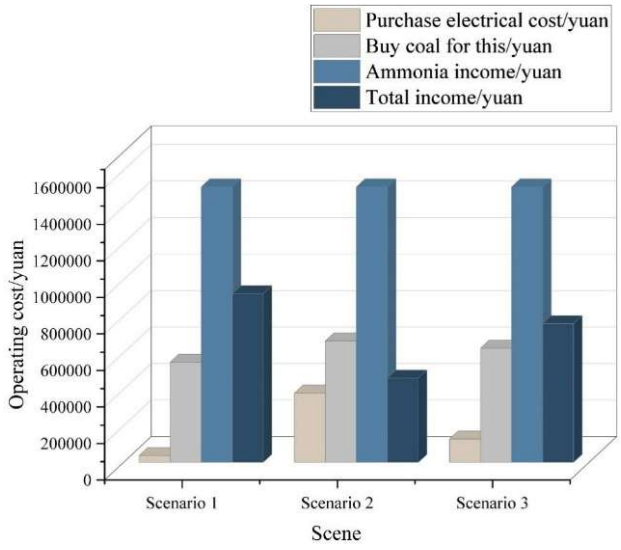

Figure 7: The operating cost comparison of three scenarios

IV. C. Method sensitivity analysis

IV. C. 1) Sensitivity analysis

Using the payback period as a measure, we focused on analyzing the impact of SOC acquisition cost, storage and transportation cost, and revenue fluctuation (unit price of hydrogen and incremental power sales) on the system operation results. When the unit price of the three segments varies at ±10% and ±20%, respectively, the payback period results change as shown in Figure 8.

The system revenue is negatively correlated with the payback period, with 20% higher revenue and 9.27% shorter payback period. The most sensitive influence on the payback period is the cost of equipment purchase, so the key to realize the centralized utilization of SOC is still to reduce the cost through the material research and development of the fuel cell industry. At the same time, due to the huge system hydrogen production, the payback period is also

more sensitive to the selling price of hydrogen, if the future price of hydrogen rises or there is a policy selling price subsidy, it will also have a very positive effect on the promotion of the application of SOC.

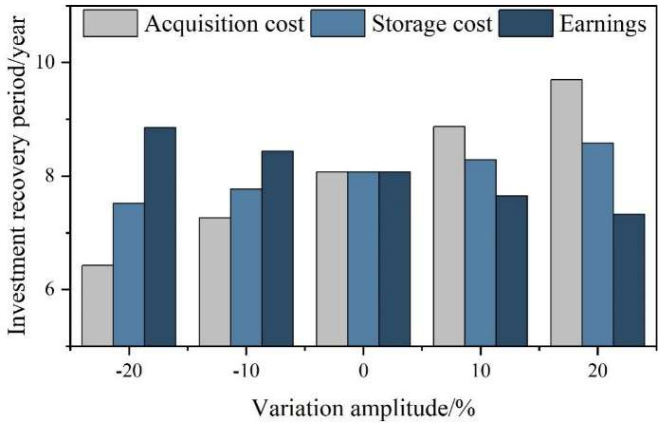

Figure 8: Payback period sensitivity comparison

IV. C. 2) Sensitivity Analysis of Wind and Light Abandonment

As the cost of abandoned wind and light has a large impact on the system economy and configuration results, and it has a large subjective influence factors, by changing the price of abandoned wind and light penalties to observe the changes in the configuration results, and carry out the analysis of the sensitivity of abandoned wind and light, and the results are shown in Fig. 9.

As the penalty price rises, the overall trend of the configuration results is upward. When the penalty price is 0, the system configuration capacity result is lower at 11.77 MW because of the higher equipment acquisition cost, and the capacity demand is reduced to improve the economy by actively abandoning wind and light, When the penalty price rises, the capacity needs to be increased to avoid the phenomenon of abandoning wind and light, and the SOC capacity is increased to about 15 MW, the configuration result can realize the full consumption of wind and light, and the raising of the penalty price no longer affects the configuration result. However, the configuration result does not increase linearly with the increase of the penalty price, because with the decrease of wind and light abandonment, the system hydrogen production and power generation increase, which means higher O&M and storage costs.

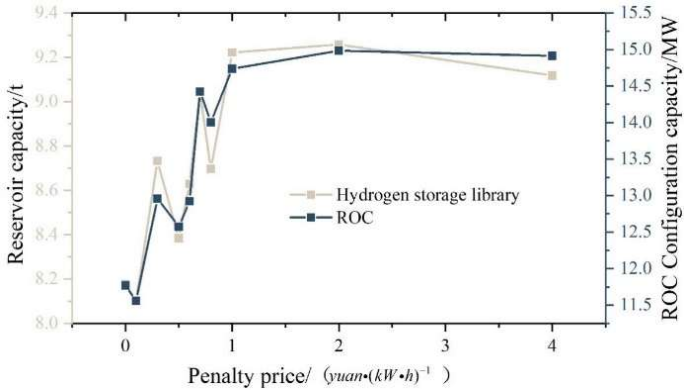

Figure 9: Comparison of price sensitivity for wind and light abandonment penalties

V. Conclusion

In this paper, different typical application scenarios of electric-hydrogen coupling are sorted out, and based on the concept of energy bus, the coupling relationship between various types of equipment in the EH-IES system is established, the model of each equipment of the system is designed, and the model is solved by the improvement of the scenario method.

(1) Analyze the wind power output of three typical application scenarios through the calculation example, in the time period of 1:00-07:00, the battery charging volume and the power input from the electrolyzer are 886.36kW and 1011.51kW, respectively. in Scenario 1, the new energy output peak is located in the morning time of 07:00-09:00

and the afternoon time of 15:00-17:00 are 169.82MW and 79.62MW, respectively: In Scenario 1, the peaks of new energy output are located at 07:00-09:00 in the morning and 15:00-17:00 in the afternoon, and the peaks of power generation are 169.82 MW and 79.62 MW, respectively.

(2) Analysis of the results of 168h optimal scheduling of the battery in different scenarios, Scenario 1 sells power to the external grid most of the time, with the highest power sale of 950 kW. whereas, in Scenario 2, the frequency of power trading leads to a substantial increase in the cost of purchasing power in the countryside, and the total benefit decreases accordingly, with the cost of purchasing power and the total benefit of 378,466 and 461,654 yuan, respectively.

(3) Using payback period as a measure to study the cycle sensitivity of electro-hydrogen coupling planning, the system return is negatively correlated with the payback period, with a 20% elevation in return reducing the payback period by 9.27%.

References

[1] Egeland-Eriksen, T., Hajizadeh, A., & Sartori, S. (2021). Hydrogen-based systems for integration of renewable energy in power systems: Achievements and perspectives. International journal of hydrogen energy, 46(63), 31963-31983.

[2] Li, Z., Zhang, W., Zhang, R., & Sun, H. (2020). Development of renewable energy multi-energy complementary hydrogen energy system (A Case Study in China): A review. Energy Exploration & Exploitation, 38(6), 2099-2127.

[3] Uyar, T. S., & Beşikci, D. (2017). Integration of hydrogen energy systems into renewable energy systems for better design of 100% renewable energy communities. International Journal of Hydrogen Energy, 42(4), 2453-2456.

[4] Zhao, S., Han, Y., Xu, Q., Wang, Z., & Shan, Y. (2024). Modeling and Simulation of Electric–Hydrogen Coupled Integrated Energy System Considering the Integration of Wind–PV–Diesel–Storage. Modelling, 5(4), 1936-1960.

[5] Zhang, Q., Qin, T., Wu, J., Hao, R., Su, X., & Li, C. (2024). Synergistic Operation Strategy of Electric-Hydrogen Charging Station Alliance Based on Differentiated Characteristics. Energy, 132132.

[6] Shi, M., & Huang, Y. (2023). Dynamic planning and energy management strategy of integrated charging and hydrogen refueling at highway energy supply stations considering on-site green hydrogen production. International Journal of Hydrogen Energy, 48(77), 29835-29851.

[7] Dai, S., Shen, P., Deng, W., & Yu, Q. (2024). Hydrogen energy in electrical power systems: A review and future outlook. Electronics, 13(17), 3370.

[8] Wan, J., Kang, J., Liu, Z., Yan, H., & Li, Y. (2024, March). Research on scenario construction and economic analysis for electric-hydrogen coupling. In Journal of Physics: Conference Series (Vol. 2728, No. 1, p. 012075). IOP Publishing.

[9] Li, J., Wang, M., Wu, Z., Tian, G., Zhang, N., & Liu, G. (2024). Optimal Operation Strategy of Electricity-Hydrogen Regional Energy System under Carbon-Electricity Market Trading. Energy Engineering, 121(3), 619-641.

[10] Wen, L., & Jiang, W. (2024). Bi-level capacity optimization of electricity-hydrogen coupled energy system considering power curtailment constraint and technological advancement. Energy, 307, 132603.

[11] Dong, H., Shan, Z., Zhou, J., Xu, C., & Chen, W. (2023). Refined modeling and co-optimization of electric-hydrogen-thermal-gas integrated energy system with hybrid energy storage. Applied Energy, 351, 121834.

[12] Ma, S., Mei, S., & Yu, L. (2023). Research on multi-timescale operation optimization of a distributed electro-hydrogen coupling system considering grid interaction. Frontiers in Energy Research, 11, 1251231.

[13] Li, H., & Zhang, J. (2024). Towards Sustainable Integration: Techno-Economic Analysis and Future Perspectives of Co-located Wind and Hydrogen Energy Systems. Journal of Mechanical Design, 146(2).

[14] Ye, J., Dong, Q., Yang, G., Qiu, Y., Zhu, P., Wang, Y., & Sun, L. (2024). Multi-objective optimal configuration of CCHP system containing hybrid electric-hydrogen energy storage system. Energy Informatics, 7(1), 1-20.

[15] Ran, L., Mao, Y., Yuan, T., & Li, G. (2022). Low-carbon transition pathway planning of regional power systems with electricity-hydrogen synergy. Energies, 15(22), 8764.

[16] Weiming, L., Jiekang, W., Jinjian, C., Yunshou, M., & Shengyu, C. (2022). Capacity allocation optimization framework for hydrogen integrated energy system considering hydrogen trading and long-term hydrogen storage. IEEE Access, 11, 15772-15787.

[17] Liu, N., Zhang, K., & Zhang, K. (2024). Coordinated configuration of hybrid energy storage for electricity-hydrogen integrated energy system. Journal of Energy Storage, 95, 112590.

[18] Pan, J., Li, R., Lei, J., Cao, Y., Chen, A., & Zhang, H. (2023, May). Research on Multi-scenario Optimization Scheduling Strategy of Electrolysis-Hydrogen Coupling System for New Power Systems. In World Hydrogen Technology Convention (pp. 215-225). Singapore: Springer Nature Singapore.

[19] Han, Z., Yuan, S., Dong, Y., Ma, S., Bian, Y., & Mao, X. (2022). Research on the Flexibility Margin of an Electric–Hydrogen Coupling Energy Block Based on Model Predictive Control. Frontiers in Energy Research, 10, 879244.

[20] Liu, X., Zu, L., Wei, Z., Wang, Y., Pan, Z., Xiao, G., & Jenkins, N. (2024). Two-layer optimal scheduling of integrated electric-hydrogen energy system with seasonal energy storage. International Journal of Hydrogen Energy, 82, 1131-1145.

[21] Wang, Y., Liu, C., Qin, Y., Wang, Y., Dong, H., Ma, Z., & Lin, Y. (2023). Synergistic planning of an integrated energy system containing hydrogen storage with the coupled use of electric-thermal energy. International Journal of Hydrogen Energy, 48(40), 15154-15178.

[22] Pan, G., Gu, W., Lu, Y., Qiu, H., Lu, S., & Yao, S. (2020). Optimal planning for electricity-hydrogen integrated energy system considering power to hydrogen and heat and seasonal storage. IEEE Transactions on Sustainable Energy, 11(4), 2662-2676.

[23] Yu, H., Chen, H., Zuo, Z., Liu, W., Ying, Y., & Ai, X. (2022, December). Optimal Planning of Power-to-Hydrogen Unit Considering Electrical-Thermal Coupling in Power System with Offshore Wind. In Frontier Academic Forum of Electrical Engineering (pp. 555-569). Singapore: Springer Nature Singapore.

[24] Deng, H., Wang, J., Shao, Y., Zhou, Y., Cao, Y., Zhang, X., & Li, W. (2023). Optimization of configurations and scheduling of shared hybrid electric-hydrogen energy storages supporting to multi-microgrid system. Journal of Energy Storage, 74, 109420.

[25] Shen, Y., Hu, X., Wang, X., Zhou, Y., Guo, W., Xia, K., & Yang, S. (2023, December). Generation Coordination and Planning of New Power System Considering Industry Hydrogen Load. In Journal of Physics: Conference Series (Vol. 2666, No. 1, p. 012034). IOP Publishing.

[26] Liu, J., Lu, C., Ma, X., Yang, X., Sun, J., & Wang, Y. (2025). Economic effects analysis model of electro-hydrogen coupling system under Energy Internet in China. Energy, 134828.
[27] Liu, Q., Huo, Q., Yin, J., Ni, J., Zhu, J., & Wei, T. (2024). Capacity Optimization and Allocation of Port Hybrid AC–DC Electric-Hydrogen Coupling System for Reduce Carbon Emissions. IEEE Transactions on Intelligent Transportation Systems.
[28] Xia, Q., Wang, Q., Zou, Y., Chi, Y., Yan, Z., Meng, Q., ... & Guerrero, J. M. (2024). Physical model-assisted deep reinforcement learning for energy management optimization of industrial electric-hydrogen coupling system with hybrid energy storage. Journal of Energy Storage, 100, 113477.
[29] Huang, J., Li, W., Wu, X., & Gu, Z. (2021). A bi-level capacity planning approach of combined hydropower hydrogen system. Journal of Cleaner Production, 327, 129414.
[30] Li, Q., Xiao, X., Pu, Y., Luo, S., Liu, H., & Chen, W. (2023). Hierarchical optimal scheduling method for regional integrated energy systems considering electricity-hydrogen shared energy. Applied Energy, 349, 121670.
[31] Yamin Yan,Yumeng Wang,Jie Yan,Haoran Zhang & Wenlong Shang. (2024). Wind electricity-hydrogen-natural gas coupling: An integrated optimization approach for enhancing wind energy accommodation and carbon reduction. Applied Energy123482-.
[32] Xianqi Li,Ye He & Maojun Li. (2024). Control Strategy for Bus Voltage in a Wind–Solar DC Microgrid Incorporating Energy Storage. Electronics(24),5018-5018.
[33] Kai Wang,Mengshang Zhao,Qinghong Tang & Ruosi Zha. (2025). Investigating effects of pitch motions on aerodynamics and wake characteristics of a floating offshore wind turbine. Energy Conversion and Management119402-119402.
[34] Hongwei Kang,Yuanhao Xu,Qingyi Chen,Zhekang Li,Yong Shen & Xingping Sun. (2024). The role of reputation to reduce punishment costs in spatial public goods game. Physics Letters A129652-.
[35] Sitong Lv,Jianguo Li,Yongxin Guo & Zhong Shi. (2019). A Typical Distributed Generation Scenario Reduction Method Based on an Improved Clustering Algorithm. Applied Sciences(20).